

Development of a Rapid Global Aircraft Emissions Estimation Tool with Uncertainty Quantification

by

Nicholas W. Simone

B.S. Mechanical Engineering
Worcester Polytechnic Institute, 2008

SUBMITTED TO THE DEPARTMENT OF AERONAUTICS AND ASTRONAUTICS IN
PARTIAL FULFILLMENT OF THE REQUIREMENTS FOR THE DEGREE OF

MASTER OF SCIENCE IN AERONAUTICS AND ASTRONAUTICS
AT THE
MASSACHUSETTS INSTITUTE OF TECHNOLOGY

February 2013

© 2013 Massachusetts Institute of Technology. All rights reserved.

Signature of Author.....

Department of Aeronautics and Astronautics

January 29, 2013

Certified by.....

Steven R.H. Barrett

Assistant Professor of Aeronautics and Astronautics

Thesis Supervisor

Accepted by.....

Eytan H. Modiano

Professor of Aeronautics and Astronautics

Chair, Graduate Program Committee

[Page Intentionally Left Blank]

Development of a Rapid Global Aircraft Emissions Estimation Tool with Uncertainty Quantification

by

Nicholas W. Simone

Submitted to the Department of Aeronautics and Astronautics
On January 29, 2013 in Partial Fulfillment of the
Requirements for the Degree of Master of Science in
Aeronautics and Astronautics
at the Massachusetts Institute of Technology

ABSTRACT

Aircraft emissions impact the environment by changing the radiative balance of the atmosphere and impact human health by adversely affecting air quality. Many tools used to quantify aircraft emissions are not open source and in most cases are computationally expensive. This limits their usefulness for studies that require rapid simulation, such as uncertainty quantification and assessment of many policy options. We describe the methods used to develop the open source Aviation Emissions Inventory Code (AEIC) and produce a global emissions inventory for the year 2005 from scheduled civil aviation, with quantified uncertainty. This is the most up-to-date openly available inventory for use in atmospheric modeling studies.

We estimate that in 2005, scheduled civil aviation was responsible for 180.6 Tg (90% CI: 136.1-232.9 Tg) of fuel burn, equating to 155.5 Tg of CO₂ as C (90% CI: 117.3-200.7 Tg) and 0.108 Tg of SO_x as S (90% CI: 0.080-0.142 Tg) emissions. 2.689 Tg of NO_x as NO₂ (90% CI: 1.761-3.804 Tg), 0.749 Tg of CO (90% CI: 0.422-1.145 Tg), and 0.201 Tg of HC as CH₄ (90% CI: 0.072-0.362 Tg) were also emitted. 92% of fuel burn took place in the northern hemisphere. Landing and takeoff operations were responsible for 9.1% of total global fuel burn, while 70.6% of fuel burn occurred above 8 km. Our total fuel burn estimate agrees within 4% of other published emissions inventories for the years 2004 and 2006, which is within the uncertainty range of the analysis.

Thesis Supervisor: Steven Barrett

Title: Assistant Professor of Aeronautics and Astronautics

[Page Intentionally Left Blank]

Acknowledgements

I would first like to thank the General Electric Company for providing the funding for me to complete my graduate work through the Advanced Courses in Engineering (ACE) program, under the supervision of Ken Gould. I am extremely grateful for this financial support.

I would like to thank my advisor, Professor Steven Barrett, for his guidance throughout my research. From the very start, he had a vision of what this project could become and the impact it could have, both of which were instrumental in how my research turned out. He was always available to give comments or suggestions, despite his busy schedule and other projects. I am also grateful for his understanding of my work schedule and priorities while I completed my research; my experience would not have been the same without this.

Thank you to Marc Stettler for his help and guidance throughout the development of v2.0 of AEIC. His experience with the LTO cycle and aircraft emissions has been invaluable throughout my research.

I must also thank Tom Reynolds, of Lincoln Labs, for his help and guidance on the operational aspects of air travel. His knowledge and work has been invaluable throughout this project.

I want to thank all of my GE colleagues for their support while I completed my degree. They were very accommodating of my school schedule and the workload I had to balance.

Thanks to everyone at the PARTNER/LAE/ICAT lab for the knowledge and insight that both enhanced my research and personal education while at MIT. In particular, I would like to thank Seb Eastham, Akshay Ashok, and Steve Yim for their help with servers, code, and helping me understand the downstream use of the results of my research.

I would like to thank my parents, Tara and Keith, and my sister, Amanda, for their continued love and support.

Last, but definitely not least, I want to thank my girlfriend, Heidi, for her love, encouragement, and understanding while I completed my degree. I know the late nights and never-ending to do lists were tough, but I would not have made it through without you! Thank you for everything. I love you so very much.

[Page Intentionally Left Blank]

Table of Contents

1. Introduction	15
1.1. Context.....	15
1.2. Purpose	16
2. Methods.....	17
2.1. Landing and takeoff (LTO) cycle.....	17
2.2. Flight scheduling.....	18
2.3. Aircraft fuel burn	18
2.3.1. Flight tracks.....	18
2.3.2. Aircraft performance.....	19
2.4. Emissions.....	20
2.5. Correction for operational inefficiencies	21
2.6. Uncertainty quantification.....	22
3. Year 2005 Emissions Inventory Results	24
3.1. Code performance.....	24
3.2. Worldwide totals	24
3.3. Spatial distribution	25
3.3.1. Global.....	25
3.3.2. Latitude.....	26
3.3.3. Longitude	27
3.3.4. Altitude	28
3.4. Fuel breakdown.....	29
3.4.1. By country of origin/destination.....	29
3.4.2. By country land border.....	32
3.5. Comparison to other inventories.....	33
4. Case Studies	35
4.1. Combustor water injection as NO _x abatement for takeoff operations	35
4.1.1. Background	35
4.1.2. Methodology.....	36
4.1.3. Results	37

4.2. Air traffic management system efficiency.....	38
4.2.1. Background	38
4.2.2. Methodology.....	39
4.2.3. Results	39
5. Conclusions	41
6. References	44

List of Figures

- Figure 1:** Column sum of global fuel burn from scheduled civil aviation for the year 2005.
..... 25
- Figure 2:** Latitudinal distribution of global emissions inventories using AEIC for the year 2005 (blue, this thesis) and published AEDT results by Wilkerson et al. (2010) (red). 26
- Figure 3:** Longitudinal distribution of global emissions inventories using AEIC for the year 2005 (blue, this thesis) and published AEDT results by Wilkerson et al. (2010) (red). 27
- Figure 4:** Altitudinal distribution of global emissions inventories using AEIC for the year 2005 (blue, this thesis) and published AEDT results by Wilkerson et al. (2010) (red). 28

List of Tables

Table 1: Summary of global emissions	25
Table 2: Total fuel burn by country of origin/destination in 2005, averaged.....	29
Table 3: Per capita fuel burn and CO ₂ emissions by country of origin/destination in 2005, averaged. Countries with populations of under 1 million have been omitted.....	30
Table 4: Fuel burn breakdown for EU	31
Table 5: Fuel burn within country land borders. Left: The ten countries with the largest amount of absolute fuel burn in 2005 (Tg). Right: The ten countries with the highest fuel burn density in 2005 (kg/km ²).	32
Table 6. Comparison of published global emissions inventories for scheduled civil aviation.....	33
Table 7. Results of water injection study.	37
Table 8. ATM system improvement opportunity for different emissions	40
Table 9. Contribution of each flight phase to inefficiency for different emissions	40

[Page Intentionally Left Blank]

List of Acronyms

AEDT	Aviation Environmental Design Tool
AEIC	Aviation Emissions Inventory Code
AFL	Above Field Level
ATC	Air Traffic Control
ATM	Air Traffic Management
BADA	Base of Aircraft Data
BC	Black Carbon
BFFM	Boeing Fuel Flow Method 2
CANSO	Civil Air Navigation Services Organization
CH ₄	Methane (used for mass basis)
CO	Carbon Monoxide
CO ₂	Carbon Dioxide
EI	Emission Index
EU	European Union
GEOS-5	Goddard Earth Observing System Model, Version 5
H ₂ O	Water (Typically as Water Vapor)
HC	Unburned Hydrocarbons
ICAO	International Civil Aviation Organization
kg	Kilogram (10 ³ grams)
km	Kilometer (10 ³ meters)
LTO	Landing and Takeoff
NASA	National Aeronautics and Space Administration
NM	Nautical Mile
NO ₂	Nitrogen Dioxide (used for mass basis)

NO _x	Oxides of Nitrogen
OAG	Official Airline Guide
OC	Organic Carbon
QUANTIFY	Quantifying the Climate Impact of Global and European Transport Systems
RVSM	Reduced Vertical Separation Minimum
SFC	Specific Fuel Consumption
SO _x	Oxides of Sulfur
S ^{VI}	SO ₃ and SO ₄
TAS	True Air Speed
Tg	Teragram (10 ¹² grams)
T/O	Takeoff
TIM	Time In Mode
UK	United Kingdom

[Page Intentionally Left Blank]

1. Introduction

1.1. Context

Aviation is currently responsible for approximately 3% of global fossil fuel consumption (IEA/OECD, 2007) and 12% of transportation related CO₂ emissions (ICAO, 2010). Global aviation traffic has grown substantially over the last several decades and is expected to continue increasing: passenger travel has increased ten-fold since 1970, doubled since 1995 (Airbus, 2012), and long term forecasts from ICAO place growth rates at up to 6.2% per year (ICAO, 2012). Emissions from aircraft consist of CO₂, CO, NO_x, H₂O, SO_x, unburned hydrocarbons (HC), black carbon (BC), and organic carbon (OC) (Lee et al., 2009). These emissions impact both air quality (causing adverse human health impacts) and the climate at regional and global scales.

Emissions from aircraft differ from other anthropogenic emission sources in that the vast majority occurs at high altitude (Olsen et al., 2012), with the exception of species associated with low thrust operation (CO and HC). The altitude of the emissions can cause a disproportionate increase in their effect on the climate, as in the case of NO_x (Gauss et al., 2006). Overall, aviation emissions make up approximately 3.5%-4.9% of the total radiative forcing due to all anthropogenic emissions (Lee et al., 2009), although significant uncertainties remain. In addition, more recent work has found that high altitude aircraft emissions perturb surface air quality. Barrett et al. (2010a) estimated that 80% of the ~10,000 premature mortalities per year due to the adverse air quality impacts from aircraft emissions come from emissions at cruise altitudes. This represents ~1% of the estimated 800,000 premature deaths due to air pollution from anthropogenic sources (Krzyzanowski & Cohen, 2008).

Due to the processes and chemical reactions that take place involving aircraft emissions, we must rely on global atmospheric models to assess their effects, requiring 4-D (3-D

and time) quantification of the emissions. The models used to develop these emissions datasets are typically high fidelity aircraft performance and emissions models, which make them computationally expensive. Many times, they are not open source, reducing the impact they can have in the research domain.

The computational intensity of models becomes important when rapid simulations are needed to assess several scenarios, or to quantify uncertainty. Due to the complexity of the systems being modeled and the lack of knowledge of the physical processes that take place, there is significant uncertainty in both the emissions estimates (Stettler et al., 2011; Lee et al., 2007) and the downstream effects of the emissions (Lee et al., 2009). This high level of uncertainty makes it paramount that uncertainty quantification is included as part of aviation impact studies. This is often computationally prohibitive with current tools and previous estimates of the uncertainty in civil aviation emissions in total have not previously been made.

1.2. Purpose

We describe the methods used and the results obtained from the Aviation Emissions Inventory Code (AEIC). AEIC was originally developed by Stettler et al. (2011) to quantify emissions and associated uncertainty from landing and takeoff operations. We extend the modeling domain to include the entire aircraft flight in order to quantify the global emissions of scheduled civil aviation for the year 2005. We reduce the modeling complexity through the utilization of assumptions in order to keep the computational intensity low enough to allow for rapid simulation of annual global emissions, allowing for uncertainty quantification through a Monte Carlo simulation. We produce the only publically available aviation emissions inventory with an emissions year within the past decade, and the first “bottom-up” estimate for the uncertainty in civil aviation emissions as a whole.

2. Methods

In this section, we provide an overview of the methods and assumptions used to calculate the global aircraft emissions inventory. When appropriate, computationally efficient assumptions have been used to reduce the computational intensity, greatly increasing the practicality of the model while maintaining its ability to adequately capture the dynamics required for a global estimate. There are two distinct areas of aircraft operations that are modeled: landing and takeoff (LTO) operations and non-LTO operations (climb to cruise, cruise, and descent). LTO emissions are modeled per Stettler et al. (2011) and are defined as those that take place between 0 and 3000 feet above field level (AFL), consistent with their approach. Cruise operations are the main focus of the methodology development and include operations above 3000 feet AFL. The areas described herein consist of an LTO cycle overview, flight scheduling, aircraft fuel burn, emissions calculations, corrections for operational inefficiencies in the system, and uncertainty quantification.

2.1. Landing and takeoff (LTO) cycle

We calculate LTO fuel burn and emissions using the methodology described in Stettler et al. (2011). A brief overview is given here. The LTO cycle is defined using specific times-in-mode (TIMs) for different portions of the cycle. ICAO has defined a default LTO cycle consisting of takeoff, climb, approach, and taxi/ground idle with specified thrust levels and times for each portion (ICAO, 2008). As defined in Stettler et al. (2011), the ICAO default cycle is typically not representative of real world operations. Thus, a more representative cycle that consists of TIMs and thrust levels for taxi out, taxiway acceleration, hold, takeoff, initial climb, climb out, approach, landing roll, reverse thrust, and taxi in has been used.

2.2. Flight scheduling

We use the Official Airline Guide (OAG) (OAG Aviation, 2005) to generate a schedule of flights for the year 2005. The OAG contains only scheduled civil air traffic; no adjustment is made to the resulting output for unscheduled or canceled flights. There is more discussion on the effect of this assumption in section 3.5.

We model traffic from 2,572 airports around the world in order to capture 99% of the passenger enplanements contained within the OAG. The OAG data is used to generate unique aircraft-airport directional pairs and calculate the number of times each pair is flown over a specified time period.

2.3. Aircraft fuel burn

2.3.1. Flight tracks

Flight tracks for each unique aircraft-airport directional pair from the OAG data are generated in order to calculate and track fuel burn and emissions for each flight. We assume all aircraft follow a great circle path between the departure and arrival airports. We reduce the absolute error introduced by using this assumption afterwards by incorporating lateral inefficiency metrics available in the literature (discussed in section 2.5).

We incorporate wind data from GEOS-5 (Rienecker et al., 2008) into the analysis. This data consists of wind direction and annually averaged wind speed. The incorporation of this data serves to change the relationship between the true air speed (TAS) and ground speed for an aircraft depending on spatial location and heading. Thus, flights with a headwind component fly slower with respect to the ground and those with a tailwind fly faster.

2.3.2. Aircraft performance

We calculate aircraft performance using EUROCONTROL's BADA (Base of Aircraft Data) Version 3.9 (Eurocontrol Experimental Center, 2011). BADA contains support for 338 total aircraft; 117 of which are "directly supported", in that their performance and operational characteristics are specifically modeled in BADA. The remaining 221 aircraft are supported by similarity to the other models, as determined by EUROCONTROL. Following the approach of Stettler et al. (2011), we estimate performance for aircraft not specified by EUROCONTROL in BADA by modeling them as other similar aircraft.

To optimize calculations in this area, we calculate aircraft performance using a pre-defined look-up table, as opposed to a physics-based aircraft performance model, which would be computationally expensive. There is a unique look-up table for each BADA supported aircraft that includes TAS, fuel flow rate, and rate of climb/descent for various flight levels and aircraft weights. This method allows fuel burn and velocity to be calculated for each flight chord using only a table look-up.

To make calculations more efficient, we simulate each unique aircraft-airport directional pair only once. Total fuel burn for a given interval is then calculated by multiplying the output from the one simulated flight by the number of times that flight operates over an interval. This allows us to estimate emissions for over 27 million flights annually using ~110,000 simulations (a 99.6% reduction), while still capturing average characteristics, as will be shown in the results.

Assumptions for aircraft takeoff weight and cruise altitude are required because FDR (flight data recorder) and radar track information are not used in the model. We utilize a takeoff weight assumption from Evers et al. (2004), which consists of the empty weight of the airframe, 60.9% of maximum payload capacity, fuel payload to fly to the destination, 5% extra reserve fuel, fuel for a diversion [100 NM (nautical miles) for short

haul and 200 NM for long haul], and fuel for a low altitude hold (45 min for short haul and 30 min for long haul) (Eyers et al., 2004). We define short haul flights as flights less than or equal to three hours in length and long haul flights as those greater than three hours. Aircraft cruise altitude is nominally set to 7,000 feet (ISA pressure altitude) below the maximum cruise altitude of the aircraft, as specified by BADA. The effects of both the takeoff weight and cruise assumptions are accounted for using uncertainty distributions (discussed later).

2.4. Emissions

We calculate emissions for all flights based on the aircraft performance calculations and the specific species emitted. For SO_x emissions, we assume a mass fuel sulfur content (FSC) of 600 ppm (Hileman et al., 2010; Stettler et al., 2011) and a 2% conversion efficiency to S^{VI} (Barrett et al., 2010b). For CO_2 , we utilize a constant emission index (EI) of 3160 g- CO_2 /kg-fuel (Stettler et al., 2011). In this manner, both SO_x and CO_2 emissions scale directly with fuel burn.

For NO_x , HC, and CO, we utilize EIs from the ICAO Engine Emissions Databank (CAA, 2009), along with Boeing's Fuel Flow Method 2 (BFFM2) (Baughcum et al., 1996) to calculate the emissions for all flights. The ICAO databank contains information on emissions and fuel flow from engines certified for flight at four different certification thrust levels: 7%, 30%, 85%, and 100%. The ICAO data is supplied at sea level, engine uninstalled conditions and adjustments are made for engine installation effects that increase fuel flow at a given thrust and altitude effects, as suggested by Baughcum et al. (1996).

BFFM2 provides a method to interpolate/extrapolate between the thrust points in the databank, as well as extrapolate the data from sea level to altitude. The interpolation

between certification points consists of a log-log linear fit for NO_x and a log-log bilinear fit for HC and CO to certification measurements. Extrapolating the emissions indices to altitude requires a correction on both the fuel flow rate from BADA, as well as a correction to the reference EIs from the ICAO databank. The fuel flow correction depends on ambient pressure, temperature, and flight Mach number. The result is a sea level, static, standard day equivalent fuel factor that can be used with the ICAO databank EIs. HC and CO EIs are then corrected for ambient temperature and pressure, while the NO_x EI is corrected for ambient temperature, pressure, and humidity level. Consistent with other studies, we assume a relative humidity of 60% for the entire flight (Baughcum et al., 1999; Kim et al., 2007; Pham et al., 2010).

2.5. Correction for operational inefficiencies

We correct the non-LTO fuel burn and emissions calculations according to lateral inefficiency factors (Reynolds, 2008, 2009). Reynolds (2008, 2009) examined several sets of flight data to determine the average increase in ground track from great circle for various flights due to factors such as route structure, air traffic control (ATC) procedures and deviations for weather and congestion. We utilize only the portion referred to as “Ground Track Extension”; that is, the added distance flown by an aircraft when compared to leaving the terminal area in a straight line, flying enroute to the arrival airport on a great circle path, and approaching the terminal area in a straight line. No adjustments are made for inefficiencies due to less than optimum cruise altitude or speed.

The lateral inefficiency factors serve to increase the amount of fuel burned and emissions for a given flight. We incorporate lateral inefficiencies from the United States and Europe. For areas other than the United States and Europe, lateral inefficiencies

from the United States are assumed. Departure and arrival inefficiencies are based on a 50 NM terminal area radius and enroute inefficiencies are with respect to a great circle, making them applicable to this analysis.

From Reynolds (2008), average departure inefficiency is approximately 8-9 NM, while average arrival inefficiencies are 27-28 NM due to vectoring and holding. Enroute extension is 5-6% of great circle distance. It should be noted that there is significant variability around these averages. As such, we only use these average inefficiencies for a nominal simulation and model the distribution around the average in our uncertainty assessment, which is discussed in the following section.

2.6. Uncertainty quantification

We make use of an uncertainty approach similar to Stettler et al. (2011), with necessary additions for the inclusion of cruise calculations into the analysis. We approximate uncertainty distributions using a triangular distribution [specified herein by (min, mode, max)] and quantify the level of uncertainty in each output by using a Monte Carlo simulation consisting of 1000 model executions. We utilize magnitudes for LTO operational (thrust levels, times in modes, etc.) and scientific (emissions indices) uncertainties from Stettler et al. (2011).

The uncertainties we take into account for the cruise modeling are cruise altitude, take-off weight, departure ground track extension, en-route ground track extension, arrival ground track extension, aircraft drag, and aircraft engine specific fuel consumption. Uncertainty ranges are discussed next.

Ground track extension uncertainties are based on data from Reynolds (2008); arrival and departure uncertainties are distributions of the extra distance flown, while en-route uncertainty is modeled with a multiplier on the nominal inefficiency. The departure

distributions are (0, 3, 20) NM for the US and (0, 5, 25) NM for the EU, while the arrival distributions are (0, 2, 75) NM for the US and (0, 22, 57) NM for the EU. Enroute multipliers are (0.25, 1, 2) for the US and (0.25, 1, 2.5) for the EU.

Variation in cruise altitude has been shown to be approximately 3000 feet for a 1σ uncertainty level (Lee, 2005; Lee et al., 2007); we use (-6750, 0, 6750) feet to represent the variation around our nominal cruise altitude assumption. We use a takeoff weight multiplier distribution of (0.7075, 1, 1.2925) to model the uncertainty in takeoff weight, which is representative of a 13% 1σ uncertainty (Lee et al., 2007).

The BADA performance model makes use of several simplifying assumptions that affect the fuel burn calculations in our analysis. Two significant assumptions are related to aircraft drag and engine specific fuel consumption (SFC). The modeling of SFC in BADA does not fully capture the dependency of aircraft engine performance on altitude and speed; thus, the 1σ uncertainty is approximately 11% (Lee, 2005; Yoder, 2007). We use a multiplier on flight fuel burn with a range of (0.7525, 1, 1.2475) to capture the uncertainty here. Similarly, for aircraft lift/drag performance, the BADA model does not fully capture the dependency on altitude and speed, yielding a 1σ uncertainty level of 14% (Lee, 2005). Here we also use a multiplier on flight fuel burn; the range is (0.685, 1, 1.315). The uncertainty levels used for cruise altitude, takeoff weight, SFC, and drag are consistent with those used in similar studies (Lee et al., 2007), although this has never been attempted fleet-wide.

We note that the uncertainty magnitudes we have accounted for capture the variation present in individual flights and will overestimate the uncertainty surrounding the fleet-wide average, as the variation on an individual basis will bound the uncertainty of the average. Results are quoted with 90% confidence intervals, unless otherwise specified, based on 1000 executions of AEIC. Nominal results are obtained from a simulation using nominal inputs.

3. Year 2005 Emissions Inventory Results

3.1. Code performance

Fast model execution times allow global fleet-wide simulations to be utilized in ways that have not been possible in the past, such as rapid policy analyses and fleet-wide uncertainty quantification. AEIC is capable of generating global emissions for a full year in approximately one hour on a single core and can be parallelized for multiple model simulations.

3.2. Worldwide totals

Table 1 contains a summary of worldwide emissions results, including uncertainties. We estimate that global fuel burn from scheduled civil aviation is approximately 180.6 Tg (90% CI: 136.1-232.9 Tg). The emissions with the largest uncertainty are HC emissions, attributable to the large amount of uncertainty that exists in the EI for HC emissions at low thrust. It should be noted that HC emissions also show the greatest amount of variability among different emissions inventory studies (Olsen et al., 2012; Kim et al., 2007). A simulation with no wind results in a fuel burn decrease of approximately 0.6%.

Table 1: Summary of global emissions

Emission	Nominal (Tg)	Mean (Tg)	Median (Tg)	Coefficient of Variation	90% Confidence Interval (Tg)
Fuel Burn	180.6	180.9	178.5	16.7%	136.1-232.9
CO ₂ as C	155.6	155.8	153.7	16.8%	117.3-200.7
SO _x as S	0.108	0.108	0.107	17.9%	0.080-0.142
NO _x as NO ₂	2.689	2.631	2.535	23.7%	1.761-3.804
CO	0.749	0.760	0.749	28.8%	0.422-1.145
HC as CH ₄	0.201	0.203	0.196	42.6%	0.072-0.362

3.3. Spatial distribution

3.3.1. Global

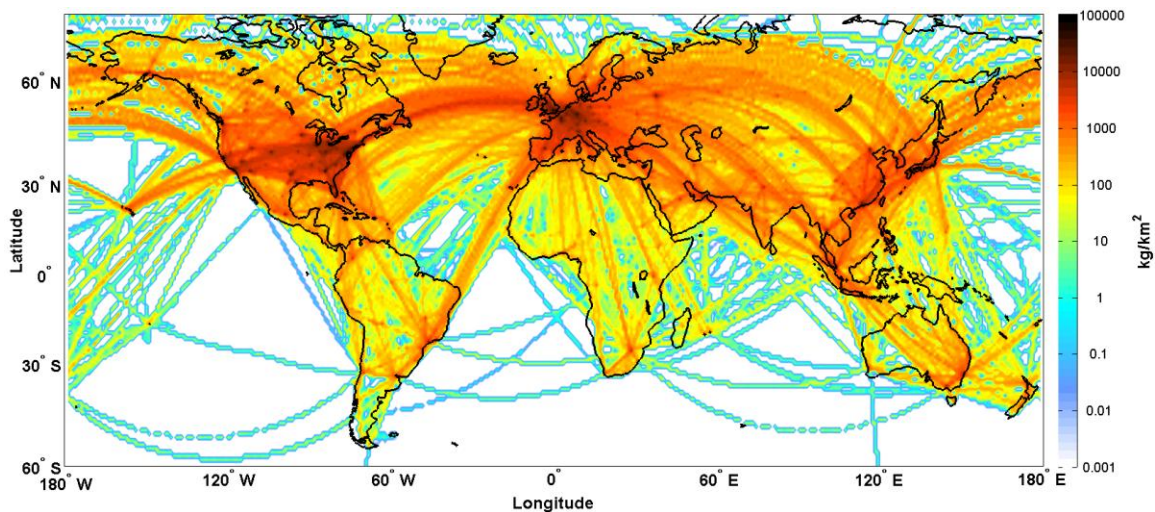


Figure 1: Column sum of global fuel burn from scheduled civil aviation for the year 2005.

Figure 1 shows the spatial distribution of global fuel burn from scheduled civil aviation for 2005. 44.5% of the globe has an annual fuel burn total of less than 1 kg/km². We note that the lack of track dispersion when generating the fuel burn totals will result in

more concentrated emissions than if the tracks are more spread out. In our analysis, we have assumed that each aircraft flies the same great circle route between airports, while actual flight tracks will have a distribution around this path due to separation requirements, weather, etc.

3.3.2. Latitude

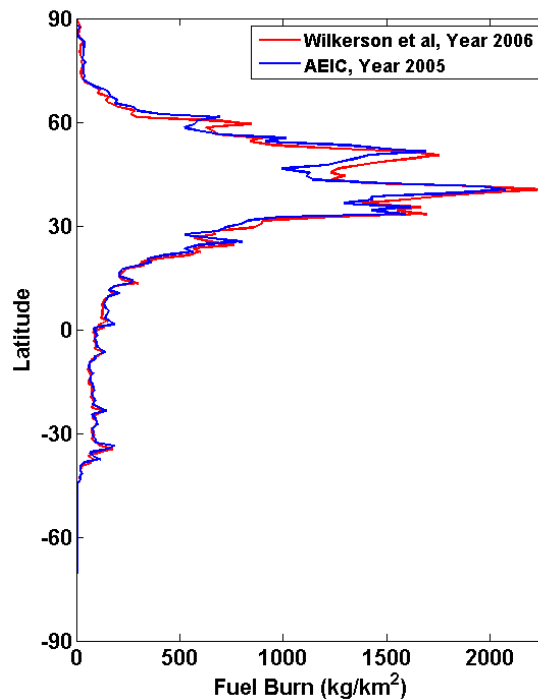


Figure 2: Latitudinal distribution of global emissions inventories using AEIC for the year 2005 (blue, this thesis) and published AEDT results by Wilkerson et al. (2010) (red).

Figure 2 contains the latitudinal distribution of fuel burn. 92% of fuel burn takes place in the northern hemisphere, with 67% percent of global fuel burn taking place in the northern mid-latitudes between 30°N and 60°N. Emissions all but cease lower than 45°S, with 0.06% of fuel burn occurring there. The largest peak occurs between 40-41°N. This peak is the result of three of the US's busiest airports being in this area (John F. Kennedy

International Airport, Newark Liberty International Airport, and LaGuardia International Airport). A comparison with AEDT results is also given.

3.3.3. Longitude

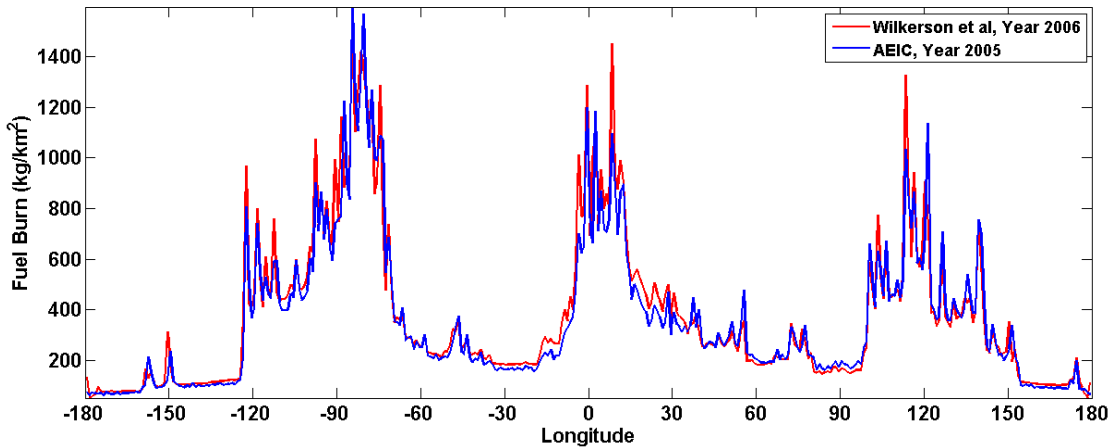


Figure 3: Longitudinal distribution of global emissions inventories using AEIC for the year 2005 (blue, this thesis) and published AEDT results by Wilkerson et al. (2010) (red).

Figure 3 contains a plot of the longitudinal distribution of fuel burn. There are three distinct peaks in the plot, corresponding to the three heaviest traffic areas in Figure 1. The peak between 120°W and 60°W accounts for 32.1% of global fuel burn and is largely a result of North American air traffic. The peak from 15°W to 30°E is a result of European air traffic, and accounts for 19.3% of global fuel burn. The last peak from 90°E to 150°E contains 21.2% of global fuel burn and is a result of the traffic in East Asia and Australia. A comparison with AEDT results is also given.

3.3.4. Altitude

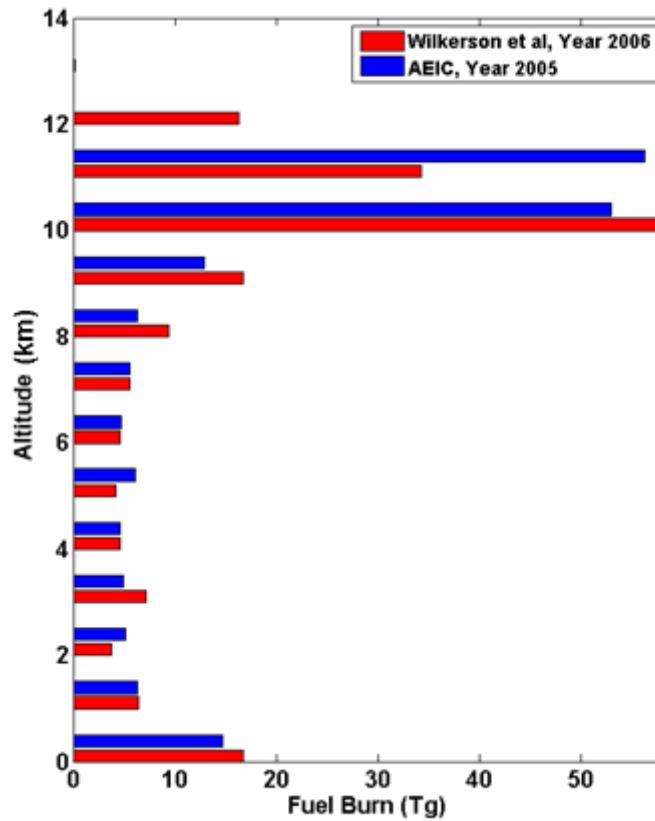


Figure 4: Altitudinal distribution of global emissions inventories using AEIC for the year 2005 (blue, this thesis) and published AEDT results by Wilkerson et al. (2010) (red).

Figure 4 shows the distribution of fuel burn with altitude. Emissions from LTO movements comprise approximately 9.1% of total global fuel burn. 70.6% of global fuel burn occurs at altitudes greater than 8 km. A comparison with AEDT results is also given.

3.4. Fuel breakdown

3.4.1. By country of origin/destination

Table 2 lists the ten countries with the highest fuel burn, based on the origin/destination of flights. The fuel burn totals for flights originating in and arriving in each country have been averaged. The proportion of fuel burn for domestic flights and international flights is also included. LTO fuel burn for all flights is counted as domestic. The United States has the largest fuel burn at 59.1 Tg (32.7% of the global total). It also has the highest percentage of domestic traffic (71%). Hong Kong has the largest percentage of fuel burn from international flights, with 94%.

Table 2: Total fuel burn by country of origin/destination in 2005, averaged.

Country	Fuel Burn (Tg)	% Of Global Total	% Domestic	% International
United States of America	59.1	32.7%	71%	29%
Japan	9.7	5.4%	40%	60%
United Kingdom	9.4	5.2%	13%	87%
China (excluding Hong Kong)	8.5	4.7%	63%	37%
Germany	6.7	3.7%	15%	85%
France	5.4	3.0%	17%	83%
Australia	4.4	2.4%	42%	58%
Canada	4.1	2.3%	45%	55%
Spain	3.9	2.2%	35%	65%
Hong Kong	3.5	2.0%	6%	94%

Table 3 contains data for the ten countries with the greatest per capita fuel burn and CO₂ emissions. These numbers are based on 2005 population statistics for each country from the United Nations (United Nations, 2011). Countries with populations under 1 million have been omitted. The United Arab Emirates and Singapore have the highest per capita fuel burn, both equating to approximately 2.4 tonnes of CO₂ per person. We note that, particularly for city-states, this is not appropriately interpreted as aviation CO₂ emissions attributed to the average resident of each country due to international passengers and visitors.

Table 3: Per capita fuel burn and CO₂ emissions by country of origin/destination in 2005, averaged. Countries with populations of under 1 million have been omitted.

Country	Fuel Burn/Person (kg/person)	Tonne-CO ₂ /Person
United Arab Emirates	764	2.4
Singapore	755	2.4
Hong Kong	518	1.6
New Zealand	255	0.8
Australia	216	0.7
United States of America	199	0.6
Netherlands	178	0.6
Cyprus	166	0.5
Mauritius	159	0.5
United Kingdom	156	0.5

Table 4 shows the fuel burn breakdown for the 27 member states of the current European Union (EU) (European Union, 2012). The largest contributor to the total EU fuel burn is the international-non LTO phase of flights, which accounts for about 73% of EU-attributed fuel burn. The total fuel burn for the EU is 59.8 Tg, which accounts for 33.1% of the global total – approximately equal to the United States. On a per capita basis, the EU as a whole consumes 121 kg/person of fuel (0.4 tonne-CO₂/person), which would place it below the Top 10 countries in terms of per capita fuel burn (Table 3).

Table 4: Fuel burn breakdown for EU

	Fuel Burn (Tg)	Contribution To Total
Domestic-Non LTO	13.0	22%
International-Non LTO	43.7	73%
LTO	3.1	5%

3.4.2. By country land border

Table 5 lists the ten countries with the highest level of absolute fuel burn and the highest fuel burn density (fuel burn per unit area) within their land borders. We have utilized the Gridded Population of the World for country land territory (CIESIN/Columbia University/CIAT, 2005). Six of the ten countries with the largest absolute fuel burn are the six largest countries in the world (United States of America, China, Russia, Canada, Australia, and Brazil). The countries with the highest fuel burn density are mostly European countries that are relatively small in size. Germany, France, Japan, and the United Kingdom appear in the top ten list of both absolute fuel burn and fuel burn density.

Table 5: Fuel burn within country land borders. Left: The ten countries with the largest amount of absolute fuel burn in 2005 (Tg). Right: The ten countries with the highest fuel burn density in 2005 (kg/km²).

Country	Fuel Burn (Tg)	% Of Global Total	Country	Fuel Burn Density (kg/km ²)
United States of America	41.1	22.8%	Belgium	14,755
China (excluding Hong Kong)	9.4	5.2%	Germany	10,713
Russia	6.9	3.8%	Switzerland	10,707
Canada	6.0	3.3%	United Kingdom	10,683
Germany	3.8	2.1%	Netherlands	10,427
France	3.7	2.1%	Japan	8,551
Japan	3.5	1.9%	United Arab Emirates	8,024
United Kingdom	2.9	1.6%	Korea	7,774
Australia	2.9	1.6%	Austria	7,112
Brazil	2.7	1.5%	France	6,695

3.5. Comparison to other inventories

Here we provide a brief comparison to other published global inventories for years close to 2005: NASA/Boeing for 1999 (Sutkus Jr. et al., 2001; Olsen et al., 2012), Quantifying the Climate Impact of Global and European Transport Systems (QUANTIFY) for 2000 (Owen et al., 2010; Olsen et al., 2012), AERO2k for 2002 (Eyers et al., 2004), and the Aviation Environmental Design Tool (AEDT) for 2004 and 2006 (Wilkerson et al., 2010). Table 6 contains a comparison of global fuel burn, NO_x, CO, and HC for all of the inventories. CO₂ and SO_x have intentionally been omitted, as they are directly proportional to fuel burn (the latter depending on the FSC assumption).

Table 6. Comparison of published global emissions inventories for scheduled civil aviation.

Emission	NASA/Boeing Year 1999	QUANTIFY Year 2000	AERO2k Year 2002	AEDT Year 2004	AEIC Year 2005 (This Thesis)	AEDT Year 2006
Fuel Burn (Tg)	136	152	156	174.0	180.6	188.2
NO _x as NO ₂ (Tg)	1.38	1.98	2.06	2.456	2.689	2.656
CO (Tg)	0.667	----	0.507	0.628	0.749	0.679
HC as CH ₄ (Tg)	0.226	----	0.063	0.090	0.201	0.098

Our total fuel burns agrees within 4% of the inventories generated by AEDT for the years 2004 and 2006, which is well within the 90% confidence interval we calculated. AEDT is a higher fidelity tool that incorporates radar track data and models each flight individually, allowing it to account for actual flight paths and unscheduled/cancelled flights. The NASA/Boeing, QUANTIFY, and AERO2k inventories agree with a general trend of increasing fuel burn each year. No inventories for the year 2005 are available for a direct comparison; however, Wilkerson et al. (2010) does qualitatively show that fuel burn for 2005 was greater than both 2004 and 2006 (Wilkerson et al., 2010). Unscheduled flights have been estimated to account for approximately 9% of global

flights annually (Kim et al., 2007), although their impact on fuel burn/emissions has not been directly quantified.

The largest relative difference between our results and the other inventories are in the CO and HC emissions. This is not unexpected, given the relatively large uncertainty in the emission of these species and their sensitivity to power setting. Based on empirical observations, we have assumed a lower thrust level for the LTO cycle than is typically used, which increases both CO and HC emissions (Stettler et al., 2011). However, our results are within 11.1% of the NASA/Boeing inventory and the relatively low CO and HC emissions from AEDT have been noted during its development (Kim et al., 2007).

For comparison of spatial distribution, we have shown our results alongside the results from AEDT 2006 in Figure 2-Figure 4 (latitudinal, longitudinal, and altitudinal) on the basis that the AEDT inventory contains the most detail related to flight altitude and location by using radar track data. In general, our results capture all of the same peaks and valleys, but are of a lower magnitude (as expected after comparing the global totals). The altitude distribution is slightly different due to the fact that our analysis has not directly incorporated radar tracks or flight data.

4. Case Studies

4.1. Combustor water injection as NO_x abatement for takeoff operations

4.1.1. Background

Here, we perform a technology assessment using AEIC. We look at the total potential benefit of using combustor water injection to lower takeoff NO_x emissions. A combustor water injection system has been chosen over a compressor misting system due to feasibility (Daggett et al., 2007). NO_x production in aircraft engines is closely linked to combustor flame temperature (Daggett et al., 2010) and increases exponentially as thrust setting increases (Baughcum et al., 1996). When water is injected into the combustor, it lowers the flame temperature and results in lower NO_x emissions; estimated magnitudes are about an 80% reduction in NO_x for a 1:1 water:fuel injection ratio (Daggett et al., 2007).

Two potential system issues with water injection systems are corrosion (if purified water is not used) and water freezing (Daggett et al., 2007). Operationally, if payload is not decreased, the weight of the water and the storage/distribution system requires more fuel per flight. In addition, the lower combustor temperature lowers the thermal efficiency of the engine. This could result in an SFC increase of 2.0% when the water injection system is being used (Daggett et al., 2010). It is the trade-off between the added weight/lower engine efficiency and a reduction NO_x EI that we wish to study.

4.1.2. Methodology

We utilize the results of a study completed by Daggett et al. (2007), where a combustor water injection system for a 747-400ER was investigated. The water injection system designed weighed approximately 750 lb. and the aircraft required 3340 lb. of water for a 1:1 water:fuel injection ratio during takeoff. To extend these results to all aircraft and determine the impact on global emissions, we make the following assumptions:

1. Water injection is used on all flights during the takeoff, initial climb, and climb out phases.
2. The water injection system weight scales linearly with aircraft empty weight.
3. For the LTO phase, the added weight due to the system and water can be represented with an increase in thrust. For the non-LTO phase, we model the added weight of the water injection system by increasing the empty weight of the aircraft.
4. The SFC increase of 2.0% is applicable to all aircraft when the water injection system is being utilized.

Based on the empty weight of the 747-400ER (from BADA), the water injection system represents an increase in empty weight of approximately 0.2%; this fraction is used for all aircraft.

To determine the thrust increase required for the weight of the water and system on the 747-400ER, we first determined the average takeoff weight for all 747-400ER flights, utilizing the takeoff weight assumption described in Section 2.3.2. Then, assuming a linear thrust increase between this nominal takeoff weight and the 747-400ER maximum takeoff weight (90% thrust for nominal weight per Stettler et al. (2011) assumption and 100% thrust for maximum weight) (British Airways/IATA, 2002), we calculate the required thrust increase to be approximately 0.2%. We utilize this thrust increase for all aircraft during the flight phases mentioned in assumption 1.

4.1.3. Results

Table 7 contains the results of the water injection simulations. LTO and global results with and without the SFC penalty described in Daggett et al. (2010) are tabulated. The global potential for NO_x reduction using this technology is 4.4%, with a potential for an extra 0.1% reduction if the SFC penalty is reduced. The benefit for LTO NO_x reduction is much larger at 59.4-59.7%. This represents a substantial reduction in the NO_x emitted in the direct vicinity of the airport.

The global fuel burn penalty for this technology is 0.1-0.2%, but the LTO fuel burn penalty could be up to 1.0%. The majority of the LTO fuel burn penalty is from the SFC reduction. The fuel penalty due to the added weight is 0.1%, which is only 10% of the total LTO fuel burn penalty. Because LTO fuel burn accounts for about 9% of total fuel (Section 3.3.4), the takeoff SFC increase has a smaller relative effect on global fuel burn than it does on LTO fuel burn.

Table 7. Results of water injection study.

Scenario	LTO Fuel Burn Change	LTO NO _x Change	Global Fuel Burn Change	Global NO _x Change
Weight Penalty Only (No SFC Penalty)	+0.1%	-59.7%	+0.1%	-4.5%
Weight + T/O SFC Penalty	+1.0%	-59.4%	+0.2%	-4.4%

4.2. Air traffic management system efficiency

4.2.1. Background

The diffusion of new aircraft technology is typically associated with long time constants. The average lifetime of one aircraft is on the order of 25-30 years (ICAO,2007) and that does not include time for the development/certification cycles. Several goals have been set for the aviation industry to reduce its environmental impact: in 2010, the Obama Administration set the goal of carbon neutral growth for aviation by 2020, based on 2005 emissions (FAA, 2012) and another industry commitment is to reduce aviation emissions by 50% by 2050 (with respect to 2005 emissions) (CANSO, 2012).

Improvements in the air traffic management (ATM) system have the unique ability to bring system wide benefits to realization. New aircraft technologies are vital to mitigating the environmental impacts of aviation as well, but the benefits are not fully realized for a long period of time and only impact one portion of the world fleet at a time. Upgrades to the ATM infrastructure and the way aircraft are operated have the potential to be far more impactful in the short-term and quicker to implement. For example, it took 11 years to have 67% of the world adopt the Reduced Vertical Separation Minimum (RVSM) standard (Kar, 2010).

Given the timeframe of the industry goals, quantifying the opportunity pool for ATM improvements is important. In addition, much of the existing ATM literature focuses on CO₂ emissions only. Quantifying the ATM impact on NO_x, HC, and CO is also important due to the human health impacts these emissions have and their dependence on engine power level (Baughcum et al., 1996), which varies during different portions of the flight. We seek to quantify the theoretical opportunity pool for each of the above emissions using AEIC.

4.2.2. Methodology

The AEIC methodology for modeling operational inefficiencies comes from Reynolds (2008, 2009) and is covered in Section 2.5. For this study, global runs were completed with and without inefficiency for each portion of the flight (departure, en-route, and arrival) active.

4.2.3. Results

Table 8 contains the improvement opportunity for each species (note that CO₂ and SO_x efficiencies would be equivalent to fuel burn), while Table 9 contains the contribution of each flight phase to the overall inefficiency for each species. The total opportunity for fuel burn reduction is approximately 6.6%. This places the fuel efficiency of the global air traffic management system at 93.4%, which is in agreement with the Civil Air Navigation Services Organization (CANSO) estimate of 92-94% (CANSO, 2012). It should be noted that this case study does not account for sub-optimal cruise altitude due to ATM system, which is estimated to be worth about 1.2% of total fuel burn (Lovegren & Hansman, 2011). The en-route phase is the largest contributor to fuel burn inefficiency.

At 6.7%, the inefficiency level for NO_x is close to fuel burn, but the contribution breakdown is different. Due to the high thrust level during the departure phase, it has a greater contribution to NO_x efficiency than the en-route phase does. Inefficiency levels for both HC and CO (15.8% and 11.2%, respectively) are greater than the fuel burn inefficiency level. This is due to the relatively large inefficiency in the arrival phase, which accounts for the majority of the inefficiency for these species. One important aspect to note is that this AEIC simulation may not fully capture the different power levels that arrival inefficiencies occur at. This study assumes the engines are a descent

power level throughout the arrival portion of the flight, while actual engine thrust is higher during maneuvers such as holding.

Table 8. ATM system improvement opportunity for different emissions

Flight Phase	Fuel Burn	NO_x	HC	CO
Departure	-2.1%	-3.2%	-0.3%	-0.5%
En-Route	-3.4%	-3.1%	-1.6%	-2.1%
Arrival	-1.1%	-0.4%	-13.9%	-8.6%
Total	-6.6%	-6.7%	-15.8%	-11.2%

Table 9. Contribution of each flight phase to inefficiency for different emissions

Flight Phase	Fuel Burn	NO_x	HC	CO
Departure	33%	48%	2%	5%
En-Route	51%	46%	10%	19%
Arrival	16%	6%	88%	77%

5. Conclusions

We have developed a methodology and open source code for calculating aircraft emissions on a global scale in a rapid manner, with quantified uncertainty. The entire flight, including both LTO operations and cruise, has been modeled. Sources of uncertainty that have been accounted for include operational factors (e.g. lateral inefficiencies and times-in-mode), scientific knowledge (e.g. emissions indices), and model fidelity (e.g. fuel flow and drag calculations).

We estimate that the worldwide fuel burn for 2005 scheduled civil aviation operations is approximately 180.6 Tg (90% CI: 136.1-232.9 Tg), equating to 155.5 Tg of CO₂ as C (90% CI: 117.3-200.7 Tg) and 0.108 Tg of SO_x as S (90% CI: 0.080-0.142 Tg) emissions. 2.689 Tg of NO_x as NO₂ (90% CI: 1.761-3.804 Tg), 0.749 Tg of CO (90% CI: 0.422-1.145 Tg), and 0.201 Tg of HC as CH₄ (90% CI: 0.072-0.362 Tg) were also emitted. The largest relative uncertainty is in HC emissions due to the uncertainty range on its emission index and its sensitivity to engine power level.

92% of fuel burn takes place in the northern hemisphere, while 67% percent of fuel burn occurs between 30°N and 60°N. Fuel burn within the longitude bands of 120°W - 60°W, 15°W - 30°E, and 90°E to 150°E accounts for 72.6% of the global total. LTO operations from aircraft at or near the surface (0-3000 feet AFL) make up 9.1% of global fuel burn, while 70.6% of fuel burn occurs at cruise altitudes (>8 km).

The United States accounts for the largest portion of global fuel burn. Hong Kong and Singapore have the high per capita fuel burn, equating to about 2.4 tonnes of CO₂ per person. 73% of fuel burn associated with the EU is due to non-LTO phases of International flights. Countries with the greatest area (e.g. United States of America, China, and Russia) have the highest level of absolute fuel burn within their borders, while smaller European countries tend to have the highest fuel burn density.

Our global fuel burn totals are within 4% of other published inventories for the years 2004 and 2006, which is within the 90% confidence interval of our analysis. The longitudinal, latitudinal, and altitudinal distributions of this thesis also agree well with other inventories. To our knowledge, this inventory is the most current emissions inventory for aviation publicly available, the only one for which the underlying code is open source, and the only to estimate emissions uncertainty fleet-wide.

Water injection has the potential to reduce the emission of NO_x during takeoff by 59.4% with a relatively small increase in fuel burn (+1.0%). When averaged over all global emissions, this equates to a NO_x reduction of 4.4% with a fuel burn penalty of only 0.2%.

Improvements in the ATM system have the potential to reduce aviation emissions. The total fuel burn improvement opportunity is 6.6%, while the potential improvement in NO_x emissions is 6.7%. The improvement opportunities for HC and CO are larger at 15.8% and 11.2%, respectively. This can be compared to the forecast annual growth rate of up to 6.2% per year (ICAO, 2012)

The development of a rapid open source emissions tool allows for full scale simulations to be used for studies where the computational time of higher fidelity models makes them impractical, such as rapid policy analyses and uncertainty analyses. It can also be used in scientific assessments. For example, AEIC is being applied in studies by Gilmore et al. (2013, forthcoming) and flight-level impacts of aircraft NO_x emissions on tropospheric ozone, and by Stettler et al. (2013, forthcoming) on black carbon emissions from aviation. The 2005 AEIC inventory has also been incorporated into the open source atmospheric chemistry transport model GEOS-Chem.

[Page Intentionally Left Blank]

6. References

Airbus, 2012. *Global Market Forecast 2012-2031*. Airbus, France.

Barrett, S.R.H., Britter, R.E. & Waitz, I. A., 2010a. Global mortality attributable to aircraft cruise emissions. *Environmental science & technology*. 44 (19). 7736–7742.

Barrett, S.R.H., Prather, M., Penner, J., Selkirk, H., Doppelheuer, A., Fleming, G., Gupta, M., Halthore, R., Hileman, J., Jacobson, M., Kuhn, S., Miake-lye, R., Petzold, A., Roof, C., Schumann, U., Waitz, I. & Wayson, R., 2010b. *Guidance on the use of AEDT Gridded Aircraft Emissions in Atmospheric Models v2.0*.

Baughcum, S.L., Begin, J. & Franco, F., 1999. Aircraft Emissions: Current Inventories and Future Scenarios. In: D. J. G. J.E. Penner, D.H. Lister (ed.). *Aviation and the Global Atmosphere*. 1999, Intergovernmental Panel on Climate Change, pp. 290–331.

Baughcum, S.L., Tritz, T., Henderson, S. & Pickett, D., 1996. Scheduled Civil Aircraft Emission Inventories and Analysis for 1992 : Database Development and Anlaysia. *NASA Contractor Report 4700*.

British Airways/IATA, 2002. Take-off at less than full power. *ICAO/CAEP/Working Group 3/AEM Task Group. June 27-28, 2002*.

CAA, 2009. *Aircraft Engine Emissions*.

CANSO, 2012. *Accelerating Air Traffic Management Efficiency: A Call to Industry*.

CIESIN/Columbia Univerity/CIAT, 2005. *Gridded Population of the World, Version 3 (GPWv3): National Identifier Grid*. Available at online: <http://sedac.ciesin.columbia.edu/data/collection/gpw-v3>. [Accessed: 6 November 2012].

Daggett, D., Hendricks, R., Mahashabde, A., & Waitz, I., 2007. Water Injection—Could it Reduce Airplane Maintenance Costs and Airport Emissions? *NASA/TM—2007-213652*.

Daggett, D. L., Fucke, L., Airplane, B. C., Hendricks, R. C., & Eames, D. J. H., 2010. Water Injection on Commercial Aircraft to Reduce Airport Nitrogen Oxides. *NASA/TM—2010-213179*.

Eurocontrol Experimental Center, 2011. User Manual for The Base Of Aircraft Data (Bada) Revision 3.9. *EEC Technical/Scientific Report No. 11/03/08-08*.

European Union, 2012. *Member states of the EU*. 2012. Available at online: http://europa.eu/about-eu/countries/index_en.htm. [Accessed: 11 December 2012].

Eyers, C.J., Norman, P., Middel, J., Plohr, M., Michot, S., Atkinson, K. & Christou, R., 2004. AERO2k Global Aviation Emissions Inventories for 2002 and 2025. *QINETIQ/04/01113*.

FAA, 2012. *United States Aviation Greenhouse Gas Emissions Reduction Plan*.

Gauss, M., Isaksen, I., DS, L. & Sovde, O., 2006. Impact of aircraft NO_x emissions on the atmosphere – tradeoffs to reduce the impact. *Atmospheric Chemistry and Physics*. 6. 1529–1548.

Hileman, J.I., Donohoo, P.E. & Stratton, R.W., 2010. Energy Content and Alternative Jet Fuel Viability. *Journal of Propulsion and Power*. 26 (6). 1184–1196.

ICAO, 2007. *Review of the Fleet and Operations Module (FOM) Assumptions and Limitations*.

ICAO, 2012. *Forecasts of Scheduled Passenger Traffic*. 2012. Available at online: http://www.icao.int/sustainability/pages/eap_fp_forecast_longterm.aspx. [Accessed: 8 November 2012].

ICAO, 2008. *ICAO Annex 16: Environmental Protection, Volume II -- Aircraft Engine Emissions*. 552.

ICAO, 2010. *ICAO Environmental Report 2010. Aviation and Climate Change*.

IEA/OECD, 2007. *IEA Energy Balance*. International Energy Agency: Paris.

Kar, R., 2010. *Dynamics of implementation of mitigating measures to reduce CO₂ emissions from commercial aviation*. MIT.

Kim, B., Fleming, G., Lee, J., Waitz, I., Clarke, J., Balasubramanian, S., Malwitz, a, Klima, K., Locke, M. & Holsclaw, C., 2007. System for assessing Aviation's Global Emissions (SAGE), Part 1: Model description and inventory results. *Transportation Research Part D: Transport and Environment*. 12 (5). 325–346.

Krzyzanowski, M. & Cohen, A., 2008. Update of WHO air quality guidelines. *Air Quality, Atmosphere & Health*. 1 (1). 7–13.

Lee, D.S., Fahey, D.W., Forster, P.M., Newton, P.J., Wit, R.C.N., Lim, L.L., Owen, B. & Sausen, R., 2009. Aviation and global climate change in the 21st century. *Atmospheric Environment*. 43 (22-23). 3520–3537.

Lee, J.J., 2005. *Modeling Aviation's Global Emissions, Uncertainty Analysis, and Applications to Policy*. MIT.

Lee, J.J., Waitz, I.A., Kim, B.Y., Fleming, G.G., Maurice, L. & Holsclaw, C.A., 2007. System for assessing Aviation's Global Emissions (SAGE), Part 2: Uncertainty assessment. *Transportation Research Part D: Transport and Environment*. 12 (6). 381–395.

Lovegren, J. A., & Hansman, R. J., 2011. *Estimation of Potential Aircraft Fuel Burn Reduction in Cruise via Speed and Altitude Optimization Strategies*. MIT.

OAG Aviation, 2005. *OAG Schedules Data*. Available at online: <http://www.oagaviation.com/Solutions/AnalysisTools/Schedules/schedules.html> [Accessed: 15 July 2010].

Olsen, S.C., Wuebbles, D.J. & Owen, B., 2012. Comparison of global 3-D aviation emissions datasets. *Atmospheric Chemistry and Physics Discussions*. 12 (7). 16885–16922.

Owen, B., Lee, D.S. & Lim, L., 2010. Flying into the future: aviation emissions scenarios to 2050. *Environmental science & technology*. 44 (7). 2255–60.

Pham, V. Van, Tang, J., Alam, S., Lokan, C. & Abbass, H.A., 2010. Aviation emission inventory development and analysis. *Environmental Modelling & Software*. 25 (12). 1738–1753.

Reynolds, T.G., 2008. Analysis of Lateral Flight Inefficiency in Global Air Traffic Management. In: *26th Congress of International Council of the Aeronautical Sciences/8th AIAA Aviation Technology, Integration & Operations Conference*. 2008, Anchorage, AK.

Reynolds, T.G., 2009. Development of flight inefficiency metrics for environmental performance assessment of ATM. *Traffic Management Research and Development*.

Rienecker, M., Suarez, M. & Todling, R., 2008. The GEOS-5 data assimilation system: Documentation of versions 5.0. 1, 5.1. 0, and 5.2. 0. *Technical Report Series on Global Modeling and Data Assimilation*. 27.

Stettler, M.E.J., Eastham, S. & Barrett, S.R.H., 2011. Air quality and public health impacts of UK airports. Part I: Emissions. *Atmospheric Environment*. 45 (31). 5415–5424.

Sutkus Jr., D.J., Baughcum, S.L. & DuBois, D.P., 2001. Scheduled civil aircraft emission inventories for 1999: database development and analysis. *NASA/CR-2001-211216*.

United Nations, 2011. *World Population Prospects: The 2010 Revision, CD-ROM Edition*. United Nations, Department of Economic and Social Affairs, Population Division.

Wilkerson, J.T., Jacobson, M.Z., Malwitz, a., Balasubramanian, S., Wayson, R., Fleming, G., Naiman, a. D. & Lele, S.K., 2010. Analysis of emission data from global commercial aviation: 2004 and 2006. *Atmospheric Chemistry and Physics*. 10 (13). 6391–6408.

Yoder, T.A., 2007. *Development of aircraft fuel burn modeling techniques with applications to global emissions modeling and assessment of the benefits of reduced vertical separation minimums*. MIT.